Applied Surface Science 268 (2013) 432–435

Contents lists available at SciVerse ScienceDirect

Applied Surface Science

journal homepage: www.elsevier.com/locate/apsusc

Supramolecular interactions of anthraquinone networks on Au(1 1 1): Hydrogen bonds and van der Waals interactions

Ji Yeon Kim[a], Won Jun Jang[a], Howon Kim[a], Jong Keon Yoon[a], Jihun Park[a], Se-Jong Kahng[a,*,1], Jhinhwan Lee[b,*,2], Seungwu Han[c]

[a] Department of Physics, Korea University, 1-5 Anam-dong, Seongbuk-gu, Seoul, 136-713, Republic of Korea
[b] Department of Physics, KAIST, Daejeon, 305-701, Republic of Korea
[c] Department of Materials Science and Engineering, Seoul National University, Seoul 151-744, Republic of Korea

ARTICLE INFO

Article history:
Received 26 September 2012
Received in revised form
20 December 2012
Accepted 21 December 2012
Available online 31 December 2012

Keywords:
Scanning tunneling microscope
Hydrogen bond
Supramolecular network
Van der Waals interaction

ABSTRACT

Intermolecular interactions of supramolecular structures were studied in anthraquinone molecules on Au(1 1 1) using scanning tunneling microscopy. Molecular chains of linear and zigzag structures were observed and explained with simple models of hydrogen bonds. In two-dimensional islands, square and chevron structures were observed, and their molecular models were reproduced by density functional theory calculations. Square structures were made of four hydrogen bonds per molecule, whereas chevron structures were explained with four hydrogen bonds per molecule and additional van der Waals interactions. Our study shows that van der Waals interactions play cooperative roles in determining the hydrogen bonded networks of the system.

1. Introduction

Molecular self-assembly is ubiquitous in biological systems due to its high efficiency and preciseness [1–3]. It can be used to fabricate functional nano-structures for electronic devices and sensors. Understanding its mechanism based on electrostatic interactions, such as hydrogen (H) bonds, van der Waals (vdW) interactions, and dipole–dipole interactions, is a big concern in current nano-science research. Different strength and directionality of intermolecular interactions induce various ordering shapes such as rectangular, honeycomb, windmill, lamella, and linear structures [4–16]. Although H-bonds are the strongest interactions, they may corporate with other intermolecular interactions. The interplay between H-bonds and vdW interactions has been studied in several acid and dendrimer molecules that are terminated with carboxylic acid for H-bonds or peripheral alkyl groups for vdW interactions using scanning tunneling microscopy (STM) [17–19]. It was reported that planar anthraquinone (AQ) molecules formed one-dimensional or hexagonal porous structures on Cu(1 1 1) with H-bonds at the low coverage (15 molecules per 1000 substrate atoms) [5,6]. With increased coverage, AQ would form close-packing structures which might require additional interactions such as vdW interactions besides H-bonds. However, a report on the close-packing AQ on metal surface is not available in literature as far as we are aware.

In this paper, we report on the role of H-bonds and vdW interactions in the supramolecular networks of AQ molecule on Au(1 1 1) using STM and density functional theory (DFT) calculations. We chose Au(1 1 1) as a substrate, because it is known to have weaker interaction between molecules and a substrate than other coinage metal surfaces such as Ag(1 1 1) and Cu(1 1 1). It was found that AQ molecules formed chain, square and chevron structures, as a result of H-bonds and vdW interactions. Atomic models for the observed structures were proposed and discussed based on DFT calculations.

2. Experimental methods

All experiments were performed using a home-built STM housed in an ultrahigh vacuum (UHV) chamber with a base pressure below 7×10^{-11} torr. The Au(1 1 1) surface was prepared from a thin film (200 nm thick) of Au on mica that was exposed to several cycles of Ar-ion sputtering and annealing at 800 K over the course of 1 h. The surface cleanliness of the Au(1 1 1) was checked by observing typical herringbone structures on the terraces in the STM images. Commercially available anthraquinone (Tokyo

* Corresponding authors.
E-mail addresses: sjkahng@korea.ac.kr (S.-J. Kahng), jhinhwan@kaist.ac.kr (J. Lee).
[1] Department of Physics, Korea University, 1-5 Anam-dong, Seongbuk-gu, Seoul, 136-713, Republic of Korea. Tel.: +82 2 3290 3109.
[2] Department of Physics, KAIST, Daejeon, 305-701, Republic of Korea. Tel.: +82 42 350 2512.

0169-4332/$ – see front matter © 2012 Elsevier B.V. All rights reserved.
http://dx.doi.org/10.1016/j.apsusc.2012.12.117

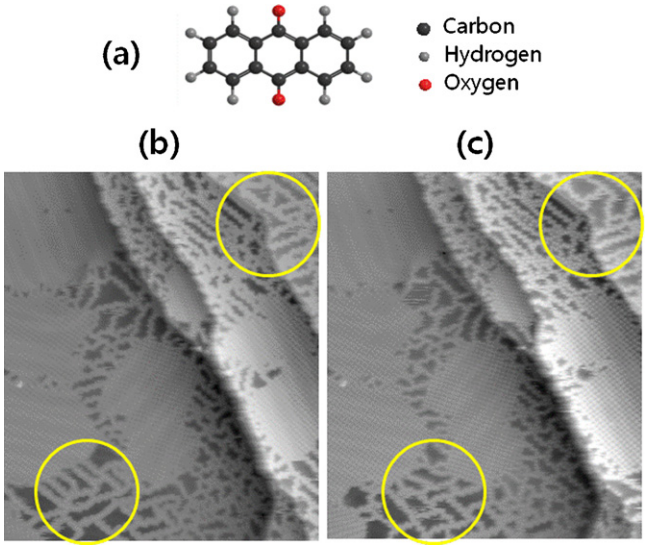

Fig. 1. (a) Atomic ball and stick model of AQ molecule. (b) An STM image obtained subsequently after AQ was deposited on Au(1 1 1). (c) An STM image obtained 3 min after the image in (b) was obtained at the same region. In (b) and (c), circles are drawn to notify the differences in the chain structures of two images. Image size: 30 nm × 35 nm. Tunneling current: I_T = 0.1 nA. Sample voltage: V_S = +0.8 V.

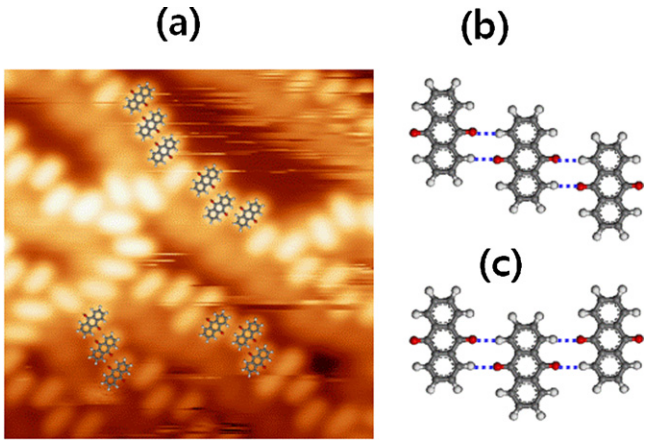

Fig. 2. (a) An STM image showing chain structures of AQ overlaid with molecular models. Image size: 8 nm × 8 nm, tunneling current: I_T = 0.1 nA, and sample voltage: V_S = +0.8. Molecular models of (b) linear and (c) zigzag structures with hydrogen bonds depicted with dotted lines.

Chemical Industry, Japan) was thermally evaporated onto the Au(1 1 1) surface at submonolayer coverage from an alumina-coated crucible, keeping the substrate temperature at 150 K. Anthraquinone molecules were outgassed for several hours prior to deposition. The prepared sample was transferred to the STM and cooled down to 80 K. The Pt–Rh alloy tip was used as an STM probe.

3. Theoretical calculations

Density functional theory calculations were performed using the VASP code [20,21]. Interaction between ions and electrons was approximated by the projector-augmented wave (PAW) potential [22]. The generalized gradient approximation (GGA) with the Perdew–Burke–Ernzerhof (PBE) functional is used to describe the exchange correlations between electrons [23]. The energy cutoff for the plane wave basis was set to 500 eV. To describe non-bonding interactions between the molecules, especially of the vdW type, an empirical scheme proposed by Grimme was adopted [24]. Square and rectangular simulation cells containing two anthraquinone molecules in the square or chevron configurations, respectively, were adopted to describe the periodic structures. The size of simulation cells, (or lattice constants) and the angular directions of two molecules in a cell were considered for calculation parameters. The height of the simulation box perpendicular to the molecule plane was fixed at 10 Å, while the lateral cell parameters were optimized such that the residual stress was reduced under 1 kbar.

4. Results and discussion

Fig. 1(a) shows the ball and stick model of AQ molecule. Fig. 1(b) and (c) show two STM images obtained subsequently at the same region, after submonolayer AQ was deposited to the substrate. The images were high-pass filtered to show the molecular structures more clearly. The images show 1-dimensional (1-d) chain structures and 2-d islands. The network configurations made of 1-d chain structures in Fig. 1(b) is different from those in (c), as denoted by the circles in the two images, whereas the shapes of 2-d islands remained mostly the same in the two subsequent STM images. The modification of chain structures seems to be induced by the tip-molecule interactions. We used typical scanning conditions of 0.8 V and 0.1 nA. The AQ molecules in chain structures must be weakly connected in comparison with those in 2-d islands. Fig. 2(a) shows a higher resolution STM image with molecular models overlaid on chain structures. A single AQ molecule had a bar-like shape with the aspect ratio of about 1:3. Chain structures have two different arrangements, linear and zigzag, as shown in Fig. 2(b) and (c), respectively. Both linear and zigzag structures are explained by two O···H bonds per molecule.

The 2-d islands in Fig. 1(b) and (c) consist of two molecular structures. Most 2-d molecular islands in Fig. 1 show the square structures, except the island at the upper left part of the image which shows chevron structures. Fig. 3(a) and (b) show high resolution STM images of square and chevron structures, respectively. Based on STM images, we propose atomic models for the two structures, which are overlaid on STM images in Fig. 3(a) and (b). Possible intermolecular interactions in the two structures are depicted with dotted lines in the atomic models in Fig. 3(c) and (d). In square structures, an AQ molecule forms eight O···H bonds with four neighboring molecules, thus four H-bonds per molecule; Two are in one molecular direction and the other two are perpendicular to the direction (the directions of unit vectors a and b in Fig. 4(a)). Similarly, in chevron structures, an AQ molecule forms eight O···H bonds with six neighboring molecules, thus four H-bonds per molecule. These clearly explain how both the square and the chevron structures are stabilized in 2d.

A DFT calculation was performed to understand the precise arrangement of AQ molecules in square and chevron structures. The calculation results, shown in Fig. 4(a) and (b), clearly reproduced the proposed models in Fig. 3. In the square structures, the long axes of two neighboring AQ molecules made a 90° angle, and the equilibrium lattice parameter, or the magnitude of the unit cell vectors, was 1.35 nm, consistent with the experimental observations (89.5° and 1.41 nm). In the chevron structures, the long axes of neighboring AQ molecules across the rows of parallel molecules formed a 116° angle. The equilibrium lattice parameters along two orthogonal directions were 1.80 nm and 0.83 nm. They are in reasonable agreement with the experimental observations (115.5°, 1.85 nm and 0.90 nm). Since the DFT results well-reproduce the model in Fig. 2, the O···H bond lengths can be extracted from the calculation results. They are 0.24 nm in the square structures, and 0.27 and 0.30 nm in the chevron structures, close to the reported sum of the vdW radii, 0.27 nm. These values imply that the O···H bonds in two structures belong to strong (0.22–0.25 nm) or

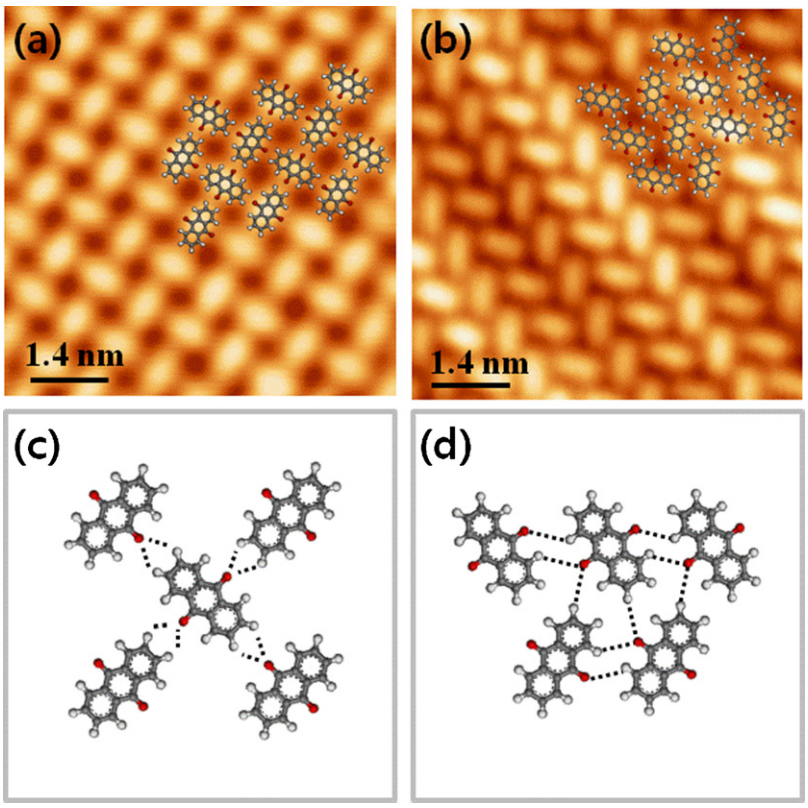

Fig. 3. STM images showing (a) square structures and (b) chevron structures. Molecular models are superimposed over the STM images in (a) and (b). In both (a) and (b) image sizes: 8.5 nm × 8.5 nm, tunneling current: I_T = 0.1 nA, and sample voltage: V_S = +0.8. Schematic illustrations for (c) four neighbor and (d) five neighbor AQ molecules from square and chevron structures, respectively. The dotted lines indicate possible H-bonds.

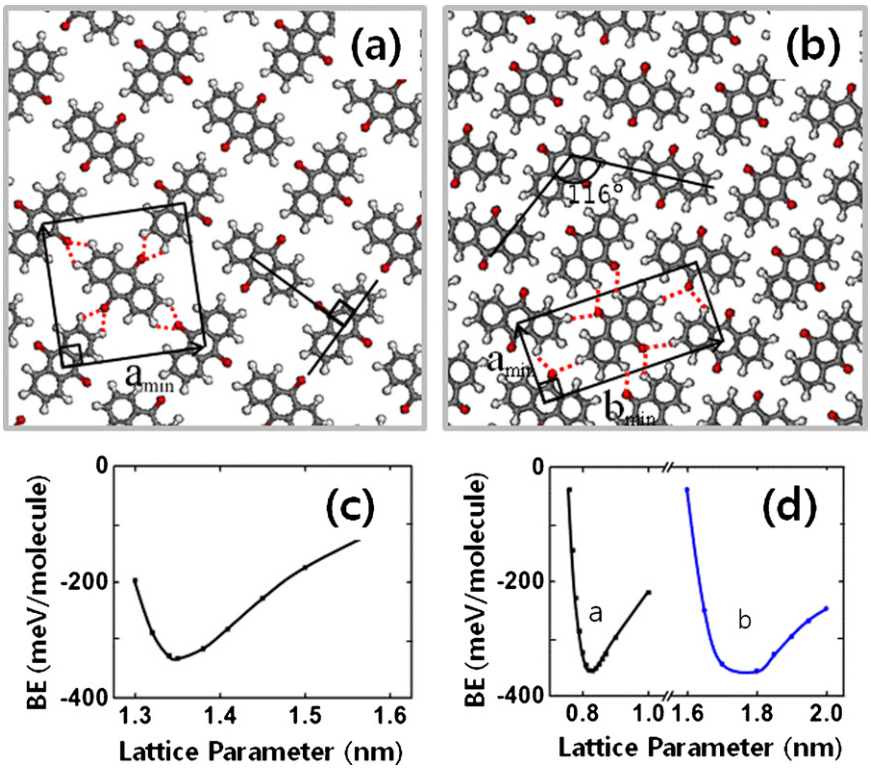

Fig. 4. The calculated results for relaxed (a) square and (b) chevron AQ structures from DFT. Unit cells are denoted with a square and a parallelogram with two unit cell vectors in (a) and (b), respectively. Possible H-bonds are drawn with dotted lines for a molecule in unit cells. The binding energies per molecule as a function of lattice parameters for (c) square and (d) chevron structures, respectively. Circles and squares are the results of the calculations and the curves represent fittings. Two graphs are selected to display for simplicity with the fixed angle and ratio between two unit vectors, although we performed calculations considering them as each independent variable.

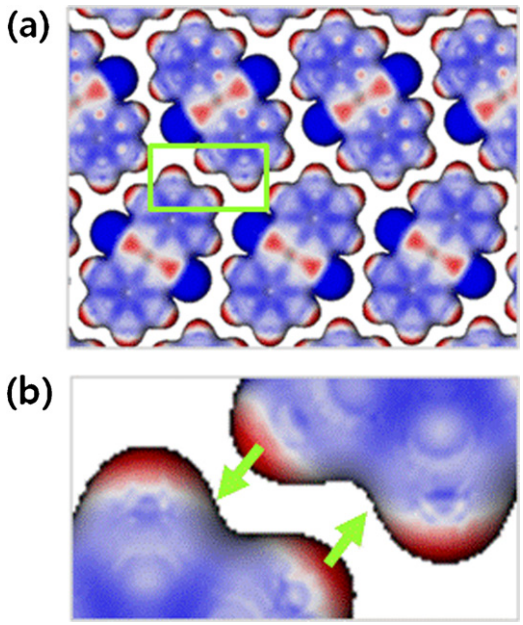

Fig. 5. (a) Chevron structures overlaid with electrostatic potential distributions. Red and blue colors correspond to positive and negative potentials. The electrostatic potential was mapped on the isosurfaces of 0.003 e/Bohr^3. (b) A zoom-in for the square region of (a). Green arrows indicate how positive potential parts are attracted by negative potential parts with van der Waals interactions. (For interpretation of the references to color in this figure legend, the reader is referred to the web version of this article.)

moderate (0.25–0.32 nm) categories of H-bonds in supramolecular structures [25].

The binding energies obtained from DFT calculations using GGA with vdW interactions were 332 meV and 367 meV per molecule for square and chevron structures, respectively, as shown in Fig. 4(a) and (b). The calculation result that the chevron structures are more stable than the square structures, is a little bit surprising. Because the square structures have much shorter H-bonds, 0.24 nm with the C—H—O angle 120° than the chevron structures, 0.27 and 0.30 nm with 122° and 180°, respectively, the square structures have stronger H-bonds than the chevron structures. The width of potential well in the potential energy curve along the direction of the unit cell vector b in Fig. 4(d) is about twice of that along the unit cell vector a in both Fig. 4(c) and (d). Such slowly varying intermolecular interactions along the unit cell vector b may be made by vdW interactions. Fig. 5 shows the molecular structures with electrostatic potential distributions. The configurations of H atoms in Fig. 5(b) show how they are arranged with vdW interactions; positive potential regions of H atoms do not make head-to-head configurations each other, but face toward negative potential regions making zipper-like structures. These vdW interactions explain how the chevron structures with weak H-bonds became more stable than the square structures with strong H-bonds. Although there were more square structures than chevron structures in Fig. 1(b), we observed that the chevron structures dominated over the square structures after thermal treatment to 300 K. This may be driven by higher energy gain in the chevron structures than in the square structures. In our calculations, substrate was not included to avoid shear calculation cost. In fact, there is a correlation between herringbone reconstructions of Au(1 1 1) and molecular structures. Namely, the direction of lattice vector a of the chevron structure was parallel to the direction perpendicular the ridge of the herringbone reconstruction or the $[11\bar{2}]$ directions of Au(1 1 1). This means that the substrate effect is not absent but seems to be cooperative to molecule-molecule interactions to form ordered networks.

5. Conclusions

We studied the supramolecular structures and their binding mechanisms of AQ on Au(1 1 1) using STM. Molecular chains of linear and zigzag structures were observed and explained with H-bonds. In 2-d islands, the square and chevron structures were observed. Their molecular models were proposed, well-reproduced, and explained by H- bonds and vdW interactions with the help of DFT calculations. Square structures consisted of four hydrogen bonds per molecule, and chevron structures were explained with four hydrogen bonds per molecule and additional van der Waals interactions. Our study shows that molecular structures with weak H-bonds per molecule can be more stable than those with strong H-bonds per molecule in the presence of other intermolecular interactions such as vdW interactions.

Acknowledgment

The authors gratefully acknowledge financial support from the Ministry of Education Science and Technology of the Korean government through National Research Foundation (2010-0025301 and 2012-0013222). SH were supported by the Center for Multiscale Energy System. This work was supported by the Supercomputing Center/Korea Institute of Science and Technology Information with supercomputing resources including technical support (KSC-2012-C2-35).

Appendix A. Supplementary data

Supplementary data associated with this article can be found, in the online version, at http://dx.doi.org/10.1016/j.apsusc.2012.12.117.

References

[1] J.W. Steed, J.L. Atwood, Supramolecular Chemistry, Wiley, Chichester, 2009.
[2] J.A.A.W. Elemans, S. Lei, S.D. Feyter, Angewandte Chemie International Edition 48 (2009) 7298.
[3] J.V. Barth, G. Costantini, K. Kern, Nature 437 (2005) 671.
[4] A. Langner, S.L. Tait, N. Lin, C. Rajadurai, M. Ruben, K. Kern, Proceedings of the National Academy of Sciences of the United States of America 104 (2007) 17927.
[5] G. Pawin, K.L. Wong, K.-Y. Kwon, L. Bartels, Science 313 (2006) 961.
[6] G. Pawin, U. Solanki, K.-Y. Kwon, K.L. Wong, X. Lin, T. Jiao, L. Bartels, Journal of the American Chemical Society 129 (2007) 12056.
[7] J.A. Theobald, N.S. Oxtoby, M.A. Philips, N.R. Champness, P.H. Beton, Nature 424 (2003) 1029.
[8] S. Weigelt, C. Busse, L. Petersen, E. Rauls, B. Hammer, K.V. Gothelf, F. Besenbacher, T.R. Linderoth, Nature Materials 5 (2006) 112.
[9] S. Buchholz, J.P. Rabe, Angewandte Chemie International Edition 31 (1992) 189.
[10] A. Marchenko, J. Cousty, L.P. Van, Lagmuir 18 (2002) 1171.
[11] F. Trixler, T. Markert, M. Lackinger, F. Jamitzky, W.M. Heckl, Chemistry: A European Journal 13 (2007) 7785.
[12] J. Schnadt, E. Rauls, W. Xu, R.T. Vang, J. Knudsen, E. Lægsgaard, Z. Li, B. Hammer, F. Besenbacher, Physical Review Letters 100 (2007) 046103.
[13] O. Ivasenko, D.F. Perepichka, Chemical Society Reviews 40 (2011) 191.
[14] T. Steiner, Angewandte Chemie International Edition 41 (2002) 48.
[15] J.K. Yoon, W.-J. Son, K.-H. Chung, H. Kim, S. Han, S.-J. Kahng, Journal of Physical Chemistry C 115 (2011) 2297.
[16] K.-H. Chung, J. Park, K.Y. Kim, J.K. Yoon, H. Kim, S. Han, S.-J. Kahng, Chemical Communications 47 (2011) 11492.
[17] K.S. Mali, K. Lava, K. Binnemans, S. De Feyter, Chemistry: A European Journal 16 (2010) 14447.
[18] P.N. Dickerson, A.M. Hibberd, N. Oncel, S.L. Bernasek, Langmuir 26 (2010) 18155.
[19] A. Cadeddu, A. Ciesielski, T.E. Malah, S. Hecht, P. Samori, Chemical Communications 47 (2011) 10578.
[20] G. Kresse, J. Hafner, Physical Review B 47 (1993) 558.
[21] G. Kresse, J. Hafner, Physical Review B 49 (1994) 14251.
[22] P.E. Blöchl, Physical Review B 50 (1994) 17953.
[23] J.P. Perdew, K. Burke, M. Ernzerhof, Physical Review Letters 77 (1996) 3865.
[24] S.J. Grimme, Computational Chemistry 25 (2004) 1463–1473.
[25] G.A. Jeffrey, An Introduction to Hydrogen Bonding, Oxford University Press, New York, 1997.